

Comparison of SUL values in oncological ^{18}F -FDG PET/CT;
The effect of new LBM formulas.

Trygve Halsne: Department of Diagnostic Physics, Oslo University Hospital, Oslo, Norway

Current address: Norwegian Meteorological Institute, Department of Ocean and Ice, Oslo, Norway

Ebba Glørsen Müller: Department of Nuclear Medicine, Oslo University Hospital, Oslo, Norway

Ann-Eli Spiten: Department of Nuclear Medicine, Oslo University Hospital, Oslo, Norway

Alexander Gul Sherwani: Department of Nuclear Medicine, Oslo University Hospital, Oslo, Norway

Lars Tore Gyland Mikalsen: Department of Diagnostic Physics, Oslo University Hospital, Oslo, Norway

Mona-Elisabeth Rootwelt-Revheim: Department of Nuclear Medicine, Oslo University Hospital, Oslo, Norway

Caroline Stokke: Department of Diagnostic Physics, Oslo University Hospital, Oslo, Norway, Department of Life Science and Health, Oslo and Akershus University College of Applied Sciences, Oslo, Norway

Author responsible for correspondence about the manuscript and to whom reprint requests should be directed:

Trygve Halsne,

Norwegian Meteorological Institute, Department of Ocean and Ice, Henrik Mohns Plass 1, 0313 Oslo, +4790823969, trygve.halsne@met.no

First author:

Trygve Halsne,

Norwegian Meteorological Institute, Department of Ocean and Ice, Henrik Mohns Plass 1, 0313 Oslo, +4790823969, trygve.halsne@met.no

Word count manuscript: 4506

Short running title: SUL in oncological ^{18}F -FDG PET/CT.

Abstract

Due to better precision and intercompatibility, the use of lean body mass (LBM) as mass estimate in the calculation of standardized uptake values (SUV) has become more common in research and clinical studies today. Thus, the equations deciding this quantity have to be verified in order to choose the ones that best represents the actual body composition.

Methods - LBM was calculated for 44 patients examined with ^{18}F -FDG PET/CT scans by means of James' and Janmahasatians' sex specific predictive equations and the results validated using a CT based method. The latter method makes use of the eyes-to-thighs CT from the PET/CT acquisition protocol and segments the voxels according to Hounsfield Units. Intraclass correlation coefficients (ICC) and Bland-Altman plots have been used to assess agreement between the various methods.

Results - A mean difference of 6.3kg (-15.1 kg to 2.5 kg LOA) between LBM_{james} and LBM_{CT1} was found. This is higher than the observed mean difference of 3.8kg (-12.5 kg to 4.9 kg LOA) between LBM_{jan} and LBM_{CT1} . In addition, LBM_{jan} had higher ICC with LBM_{CT1} of $r_I = 0.87$ ($r_L = 0.60$, $r_U = 0.94$) than LBM_{james} with $r_I = 0.77$ ($r_L = 0.11$, $r_U = 0.91$). Thus, we obtained better agreement between and LBM_{jan} and LBM_{CT1} . Although there were exceptions, the overall effect on SUV values was that SUV_{james} values were greater than SUV_{jan} values.

Conclusion - From our results, we have verified the reliability of the LBM_{jan} suggested formulas with a CT derived reference standard. Compared with the more traditional and available set of equations LBM_{james} , the LBM_{jan} formulas tend to yield better agreement.

Keywords

Standardized Uptake Value, Lean Body Mass, PET/CT, CT-based Segmentation

Introduction

The number of PET/CT investigations has increased for various oncology applications, including lung cancer investigations. PET allows noninvasive quantitative assessment of biochemical and functional processes, and standardized uptake value (SUV) is a common quantitative measure used in clinical studies and research. In general, SUV is defined as the ratio of the radioactive concentration measured in an area of interest to the injected activity divided by a mass estimate for the total distribution volume of the injected activity. The value reads

$$\text{SUV} = \frac{c_{AOI}}{A_{inj}} m_e, \quad (1)$$

where c_{AOI} is the concentration in an area of interest, A_{inj} is the injected activity corrected for decay and m_e is a mass estimate for the total distribution volume of the activity. In clinical practice and tradition, body weight (bw) is often used as mass estimate. Thus, the value is denoted SUV, which also is made unitless assuming that the patient has homogeneous mass density of $1 \frac{g}{ml}$.

In ^{18}F -fluorodeoxyglucose (^{18}F -FDG) PET/CT, several studies have reported SUV's strong correlation with body weight due to the lack of body composition and body size information (1, 2, 3). It is common knowledge that adipose tissue metabolizes far less ^{18}F -FDG than other tissue in the fasting state, and consequently adipose patients may score different SUV values than lean patients for the same tumor uptake (4, 1, 2). Therefore, alternative methods propose to use lean body mass (LBM) as mass estimate in equation (1). SUV values using LBM as mass estimate is referred to as SUL, to distinguish it from SUV.

LBM consists of the body cell mass and the nonfatty intercellular connective tissue, e.g. tendons, ligaments etc. (5). Traditionally, body fat quantification is carried out by means of skin-fold measurements and bioelectrical impedance analysis. Nowadays, non-invasive imaging techniques are considered as the gold standard for body composition and anthropometric analysis (6). Computed tomography (CT), magnetic resonance imaging and dual-energy x-ray absorptiometry are the most frequently used modalities for this purpose (7).

Since CT based methods are currently not applicable for clinical examinations, LBM is calculated from predictive equations by means of parameters as e.g. sex, height and body weight (8). A common set of equations in modern scanners is referred to as the *James equations*. They were developed based on skin-fold measurements and calculate LBM as

$$\text{LBM}_{\text{james}} = \begin{cases} 1.1 bw - 128 \left(\frac{bw}{h}\right)^2, & \text{for men,} \\ 1.07 bw - 148 \left(\frac{bw}{h}\right)^2, & \text{for women,} \end{cases} \quad (2)$$

where bw is body weight and h height (9). *James'* formalism has a well known weakness resulting in a negative correlation with body mass index (BMI) defined as bw/h^2 (10). Janmahasatian et al. (11) used another approach and developed predictive equations based on bioelectrical impedance analysis. In this method, the total body water is assumed to be a constant fraction of fat free mass (FFM), such that fat free mass can be estimated from the ratio of total body water to the constant water fraction from the impedance

index. In contrast to LBM, fat free mass does not include fat in cell membranes which makes them slightly different (5), but for simplicity we denote the equations with LBM. The equations, which they verified with dual-energy x-ray absorptiometry measurements, read

$$LBM_{jan} = \begin{cases} \frac{9.27 \times 10^3 bw}{6.68 \times 10^3 + 216 \text{ BMI}}, & \text{for men} \\ \frac{9.27 \times 10^3 bw}{8.78 \times 10^3 + 244 \text{ BMI}}, & \text{for women.} \end{cases} \quad (3)$$

In general, basing predictive equations on the present demography is found to be a complicated task due to e.g. ethnic and epoche differences (12). Hence, an effort has been laid down to extract LBM for SUL calculations by means of CT (13). The basic idea behind these methods is to decide LBM by using the already existing CT for attenuation correction (AC) purpose from the PET/CT examination on the fly.

Chan (13) developed a technique to estimate LBM from a limited field of view (FOV) CT and found that the CT computed LBM was more accurate than results obtained from predictive equations. The reliability of his method was confirmed in a later study by comparing the results with five predictive equations (14). Another group concluded that there are substantial discrepancies between individual LBM from CT and predictive equations by comparing four sets of predictive equations with CT computed LBM using a built-in software package from Siemens[®] to extract adipose tissue and adipose tissue-free body mass (15). The CT based method developed by Hamil et al. has several similarities with the method developed by Chan (13), but differs in some aspects e.g. the introduction of a skin component in order to address partial volume effects.

This study aimed to compare SUL values from the two sets of predictive equations, LBM_{james} and LBM_{jan} (i.e. eqs. 2, 3), with CT based SUL methods by means of statistical analysis. LBM_{jan} constitutes the new EANM guidelines for LBM calculations (16), and are to the authors' knowledge not previously compared and validated with a CT based method for LBM.

Materials and Methods

Patient population

A total number of 44 patients were included in the present prospective study. Consecutive patients referred for lung cancer assessment were asked to participate. Patient characteristics are listed in Table 1. The institutional review board approved this study and all subjects signed a written informed consent. The patients were selected according to their BMI in order to obtain approximately 15 subjects in each of the

intervals $[18.5, 25.0)$, $[25.0, 30.0)$ and $[30.0, \infty)$. Exclusion criteria were patients with large metal implants, proven diabetes and blood glucose higher than 8.3 mMol/l (16).

PET/CT acquisition protocols

For PET/CT image acquisition, we used a Siemens Biograph 64 (Erlangen, Germany). The patients fasted for at least 6 hours before scanning. The amount of injected ^{18}F -FDG was based on the patient's age and body weight (17). 60 minutes after injection, the patients were scanned. The CT acquisition parameters were 120 kV, 3.0 mm slice thickness, 50 mAs with a 1.35 pitch using a B31f kernel for the reconstructed CT. In the PET protocol, we scanned 3 min/bed using ordered-subsets expectation maximization algorithms with 4 iterations and 8 subsets in the reconstruction creating a 168×168 matrix smoothed with a 5.0 mm Gaussian filter.

Area of interest definition in determination of SUV

Maximum standardized uptake value (SUV_{max}) and peak SUV (SUV_{peak}) of the lesions and average SUV (SUV_{mean}) and standard deviations of the liver, were measured and registered by using a Siemens SyngoVia workstation (version VB10A, Erlangen, Germany). SUV_{max} and SUV_{peak} were measured manually, by placing a volume of interest (VOI) over target lesions. SUV_{peak} was defined as a volume of 1cm^3 around the SUV_{max} . All chosen lesions were evaluated as pathological by a nuclear medicine physician. Liver background uptake was measured by placing a region of interest of 3 cm in the right liver lobe according to the PERCIST criteria (4). Cross-sectional regions were displayed in axial, sagittal and coronal projections and controlled that there was no hypermetabolic uptake included in the reference regions. Target lesions were defined as tumor in the lung parenchyma (for 39 patients) and if more than one we included the one with the highest ^{18}F -FDG uptake. In some of the patients there were no evidence of lung tumor. In those instances we applied a VOI over the most hypermetabolic mediastinal or hilar lymph node (three patients). In one patient we placed a VOI in hypermetabolic pleura as this was the only finding. If no evidence of either lung tumor, hypermetabolic pleura or lymph node no VOI was applied (one patient).

Data analysis

LBM_{james} (eq. (2)) is calculated using bw in $[kg]$ and h in $[cm]$. For the calculation of LBM_{jan} , h have units of $[m]$ in the computation of BMI.

The CT based method developed by Hamil et al. (18) makes use of the eyes-to-thighs CT from the PET/CT

acquisition protocol. Their CT1 and CT2 method are based on estimates of lean tissue, fat and bone from counting all voxels in a characteristic range of Hounsfield Units, multiplied with voxel size and a characteristic density. An example of how the segmentation process takes place in a single axial image is shown in Figure 1. The LBM formalisms reads

$$LBM_{CT1} = bw \left(\frac{lean + bone}{lean + fat + bone} \right), \quad (4)$$

$$LBM_{CT2} = m_1 + (bw - m_2) \frac{lean + k_{fat} \times fat}{lean + fat + bone}, \quad (5)$$

where m_1, m_2 represents the brain and head mass respectively in $[kg]$, k_{fat} is a proportionality constant representing the relative uptake in fatty tissue to lean tissues. $lean, fat, body$ represent the weight ($[kg]$) of lean and fatty tissues and bone respectively. In contrast to the more intuitive LBM_{CT1} , LBM_{CT2} is meant to model the body's processing of FDG. Due to the limited CT FOV, m_1, m_2 and k_{fat} are estimated parameters.

Both the predictive equations and the CT based method were implemented using Python programming language (Python Software Foundation, version 2.7, <http://www.python.org>) along with the statistical analysis. The implementation of the CT based method was verified by a head-to-toe CT where the entire patient was within the FOV, and the patient's body weight was compared in the same way as in (18) where

$$CT_{me} = lean + fat + bone. \quad (6)$$

The difference between actual body weight and CT_{me} was of on the order of a tenth of a kg which is considered a satisfying result, implying that the method is correctly implemented.

All SUL values are calculated as

$$SUL_i = \frac{SUV_{bw}}{bw} LBM_i \quad (7)$$

where subscript i denotes the four various LBM calculations from equations (2), (3), (4) and (5).

Statistical Analysis

For continuous variables, the mean +/- standard deviation is reported. The Bland Altman analysis investigates the absolute difference between two methods (19). The average difference (bias) and the limits of

agreement (LOA), between which 95 % of all comparisons lie, are reported. In addition, intraclass correlation coefficients (ICC), r_I , are used to assess agreement between the various methods. The 95 % confidence intervals for this analysis are reported as r_L and r_U where subscript L and U denotes lower and upper respectively. This method reveals the agreement between different types of measurements (20). In all cases, LBM_{CT1} is used as reference standard. The normality of the distribution of values was graphically checked. 95 % confidence intervals are used and referred to as CIs.

Pearson correlation coefficients, r , and regression lines are computed for SUL liver values vs BMI and SUL tumor max and peak values are presented using bar plots. A paired sample t-test was used to compare the differences in tumor value results based on predictive equations.

Results

Figure 2 presents the various LBM methods compared by means of Bland-Altman plots. The mean difference and LOA are computed for both genders together.

We find good agreement between LBM_{james} and LBM_{jan} , especially for males (Figure 2A). For females, LBM_{james} introduces a systematic overprediction compared with LBM_{jan} close to 5 kg. The negative outlier is a result of a female patient with BMI = 42.

When compared directly to CT derived LBM (Figure 2C and 2D), we observe a bias in the direction of LBM overestimation for both LBM_{james} and LBM_{jan} compared with LBM_{CT1} of 6.3 kg and 3.8 kg, respectively. The LOA are of the approximate same size (CI = 8.8 kg and CI = 8.7 kg for LBM_{james} and LBM_{jan} respectively), showing that the inter-patient variation is about the same. The ICC values shown in Table 2 yield similar results with $r_I = 0.87$ ($r_L = 0.60$, $r_U = 0.94$) for LBM_{jan} and $r_I = 0.77$ ($r_L = 0.11$, $r_U = 0.91$) for LBM_{james} .

The impact of each method on measured tumor SUL values, was investigated for each patient individually. The SUL tumor peak- and max-values, computed for all patients using the three LBM formulations in equations (2), (3) and (4), are shown in Figure 3.

The overall trend is that SUL_{james} is greater than SUL_{jan} , which again is greater than our chosen gold standard method, SUL_{CT1} . There are however exceptions. The inter-patient variation is greater than the method differences. The direct impact on SUL values was for $SUL_{t,max}$ in the range (0.0, 1.3), with a median of 0.64 and for $SUL_{t,peak}$ in the range (0.0, 1.2), with a median of 0.58, for SUL_{james} compared

to SUL_{jan} . No significant differences between SUL_{jan} and SUL_{james} in relation to SUL_{CT1} were found ($P > 0.05$ for peak values and max values).

In Figure 4, SUL and SUV mean liver values are plotted against BMI together with an associated linear regression line. This shows the impact of BMI on the computed uptake values. The mean liver SUV values, range:(1.70, 2.87), were within the range in accordance to EANM guidelines (16).

Two methods for CT-derived LBM were implemented. These were compared and the results (Figure 2B and Table 2) show only a modest disagreement: $r_I = 0.98$ ($r_L = 0.89$, $r_U = 0.99$), bias -1.5 kg and -4.8 kg to 1.8 kg LOA.

Our dataset included four patients with metal implants. Three patients had a hip replacement and one had a pacemaker. In the case of pacemaker, the difference in removing six partial distorted axial planes in the middle of mediastinum was 0.1 % for LBM_{CT1} and therefore of very little concern. In the case of hip replacements, the image distortion did not affect the entire image, but we chose to exclude the axial planes of the CT series that had the metal implant. For these patients, the largest observed difference in LBM_{CT1} was 2.4 % with 48.1 vs. 49.2 kg and was considered negligible.

Discussion

Both LBM_{james} and LBM_{jan} use different equations for males and females. Our results show a systematic difference between LBM_{james} and LBM_{jan} for the female equations, while the results for the male patients are in relatively good correspondence. Consequently, changing from LBM_{james} to LBM_{jan} will most strongly affect female patients.

It is to be expected that patients with very high BMI show up as outliers in the results, when LBM_{james} and LBM_{jan} are compared directly. This is a consequence of the James equations, which have a known negative bias for high BMI patients, originating from the parabolic nature of the equations (10). The female equation obtains its maximum when $BMI \simeq 37$. After that point, LBM will decrease with increasing BMI. This is also the case for males, but with a higher maximum, $BMI \simeq 43$. In their paper, Tahari et al. (10) argues for the replacement of LBM_{james} with LBM_{jan} due to significant difference for high BMI patients, but their lack of quantitative comparison between LBM_{james} and LBM_{jan} does not reveal the method difference in the lower BMI regions. Although the Pearson correlation coefficients for SUV and SUL vs bw were lower for LBM_{jan} compared with LBM_{james} , LBM_{jan} was not validated as a reliable measure for true LBM.

As reported, we observe a bias in the direction of LBM overestimation of both LBM_{james} and LBM_{jan} compared with LBM_{CT1} of 6.3 kg and 3.8 kg respectively. The lower bias for LBM_{jan} makes this the preferred method. The ICC values shown in Table 2 yields the overall same results as the Bland-Altman analysis, i.e. LBM_{jan} have better agreement with LBM_{CT1} compared with LBM_{james} . $r_1 = 0.87$ for LBM_{jan} shows better agreement in terms of extent of correspondence between the methods than LBM_{james} , with $r_1 = 0.77$.

Decazes et al.(14) used the same statistical techniques, i.e. Bland-Altman plots and ICC, to verify Chan’s CT models, but seemingly implemented LBM_{james} wrong using 120 instead of 128 in the second term for males and h instead of bw for the first term for females. Hence, their results may not be comparable. Both their comparison with other equation-based methods and the comparisons made in Erselcan et al.(12) find discrepancies with a reference standard, using dual-energy x-ray absorptiometry in the latter case. The general trend is: If the mean values from a Bland-Altman analysis are smaller, it comes with the cost that the equations overestimates for the leanest patients and underestimates for the fattier patient, leaving us with a biased function. In the cases without a biased function, the LOAs are of about the same size as for LBM_{james} in these studies.

The positive outlier in Figure 2B to 2D is due to a subject with large muscular mass with low percentage of fat. It is to be expected that predictive equations that use BMI as a measure of fat content have difficulties estimating LBM in these types of patients.

We considered the LBM_{CT} methods as golden standard in our analysis based on multiple studies (14, 13, 2, 6), although, there are a number of variations within these CT based methods, including differences in Hounsfield Units range and tissue densities. Besides these, Decazes et al. (14) argues that the non-uniform tissue distribution in Chan’s method reflects the reality better than the uniform distribution of fat, lean and bone used in LBM_{CT1} . On the other hand, LBM_{CT2} is ment to consider the case of non-uniform distribution, introducing tracer uptake in fat and different fat content in the head. There are differences in LBM calculations from the various CT methods. Although, they are smaller compared with predictive equations. Hence, we included the LBM_{CT2} method in our study and observed a good correspondance between the two CT based methods. In comparison, LBM_{CT2} also tells us something about the uncertainty of the limited FOV in LBM_{CT1} . Less bias and high ICC, -1.5 kg and 0.98 ($r_L = 0.89$, $r_U = 0.99$) respectively, confirms the robustness of the latter method. Since LBM_{CT2} is not considered validated according to the author (18), we have performed the SUL analysis using CT1 as reference.

Metal implants is a challenge while using CT for LBM. Increase in BMI also tend to correlate with the number of people having metal implants as a result of overuse injuries. But based on our experience, the CT based methods yield more consistent results than the predictive equations for this group. In accordance to Hamil et al. (18), the change was smaller for LBM_{CT2} . This also corresponds to earlier studies where CT methods find good agreement across variations in FOV (14). Another challenge for CT based methods is the presence of large volume ascites, pleural effusions or soft tissue edema. Here, one could experience a relative bias in the direction of overestimating LBM values since these regions will falsely be characterized as lean tissue while most often having no FDG uptake. That said, the predictive equations using parameters as body weight, height etc. would also struggle with these types of volumes. In our patient population, none of the above mentioned volumes were present.

The results from our SUL computations in Figure 3 underscores the result from Figure 2, that LBM_{james} in general overpredict LBM compared with LBM_{jan} and LBM_{CT1} . The only case where the opposite is evident from Figure 3 (one patient with BMI = 25), i.e. SUL max and peak values are higher for SUL_{CT1} compared with SUL_{james} and SUL_{jan} , is the same case as stated earlier: the muscular subject with low fat percentage compared with the others. None of these patients would be diagnosed differently based on the results from the three LBM formulations, since the diagnosis often is based on the overall evaluation and not on SUL alone. Although, it is obvious that more precise SUL values will contribute to better patient diagnostics and treatment evaluation in the long term.

The results from Figure 4 is a classical way to evaluate results by means of BMI vs. SUL liver plots with associated regression lines, which ideally should be uncorrelated. In contrast to the results from Tahari et al. (10), we systematically find negative correlation for females in both SUL_{james} and SUL_{jan} (Fig. 4A and 4B). That said, the overall results are about the same. It is also worth mentioned that the number of patients in the compared study is significantly higher (i.e. 1033 vs. 44) with emphasis on patients with BMI < 30. However, as argued earlier, the lack of direct quantitative comparison between the methods makes this study important in terms of validation.

Conclusion

We have verified the reliability of the LBM_{jan} suggested formulas with a CT derived reference standard. From our results, we found that LBM_{jan} tends to yield better agreement with a CT based method, especially for females, than LBM_{james} , which is the most available SUL formulation used today. It is anticipated that

the new LBM adjusted SUV, which is also recommended from the EANM guidelines for tumor imaging version 2.0, can improve the accuracy and consistency of SUL calculations in research and clinical practice.

Disclosure

No potential conflict of interest relevant to this article was reported.

Acknowledgements

We greatly appreciate the assistance from the nuclear medicine technicians at Rikshospitalet, Oslo University Hospital.

References

- [1] Zasadny ZK, Wahl RL. Standardized uptake value of normal tissue at PET with 2-[fluorine-18]-fluoro-2-deoxy-D-glucose: variations with body weight and a method for correction. *Radiology*. 1993;189:847-850.
- [2] Kim CK, Gupta NC, Chandamouli B, Alavi A. Standardized uptake values of FDG: Body surface area correction is preferable to body weight correction. *J Nucl Med*. 1994;35:164-167.
- [3] Sugawara Y, Zasadny ZK, Neuhoff AW, Wahl RL. Reevaluation of the Standardized Uptake Value for FDG: Variations with Body Weight and Methods for correction *Radiology*. 1999;213:521-525.
- [4] Wahl RL, Jacene H, Kasamon Y, Lodge MA. From RECIST to PERCIST: Evolving Considerations for PET Response Criteria in Solid Tumors *J Nucl Med*. 2009;50:122S-150S.
- [5] Roubenoff R, Kehayias JJ. The Meaning and Measurement of Lean Body Mass *Nutr Rev*. 1991;49:163-175.
- [6] Heymsfield SB, Gonzalez MC, Lu J, Jua G, Zheng J. Skeletal muscle mass and quality: evolution of modern measurement concepts in the context of sarcopenia *Proc Nutr Soc*. 2015;74:355-366.
- [7] Kullberg J, Brandberg J, Angelhed J-E, et al. Whole-body adipose tissue analysis: Comparison of MRI, CT and dual energy X-ray absorptiometry *Br J Radiol*. 2009;82:123-130.
- [8] Deurenberg P, Weststrate KA, Seidell JC. Body mass index as a measure of body fatness: age- and sex-specific prediction formulas *Br J Nutr*. 1990;65:105-114.

- [9] James WPT, Waterlow JC, Obesity Research DHSS/MRC Group. *Research on obesity : a report of the DHSS/MRC group*. No. 0114500347 London : Her Majesty's Stationary Office 1976.
- [10] Tahari AK, Chien D, Azadi JR, Wahl RL. Optimum Lean Body Formulation for Correction of Standardized Uptake Value in PET Imaging *J Nucl Med*. 2014;55:1481-1484.
- [11] Janmahasatian S, Duffull SB, Ash S, Ward LC, Byrne NM, Green B. Quantification of Lean Bodyweight *Clin Pharmacokinet*. 2005;44:1051-1065.
- [12] Erselcan T, Turgut B, Dogan D, Ozdemir S. Lean body mass-based standardized uptake value, derived from a predictive equation, might be misleading in PET studies *Eur J Nucl Med*. 2002;29:1630-1638.
- [13] Chan T. Computerized Method for Automatic Evaluation of Lean Body Mass from PET/CT: Comparison with Predictive Equations *J Nucl Med*. 2012;53.
- [14] Decazes P, Métivier D, Rouquette A, Talbot J-N, Kerrou K. A Method to Improve the Semi-quantification of ^{18}F -FDG Uptake: Reliability of the Estimated Lean Body Mass Using the Conventional, Low-Dose CT from PET/CT *J Nucl Med*. 2016;57.
- [15] Kim CG, Kim WH, Kim MH, Kim D-W. Direct Determination of Lean Body Mass by CT in F-18 FDG PET/CT Studies: Comparison with Estimates Using Predictive Equations *Nucl Med and Mol Imaging*. 2013;47:98-103.
- [16] Boellaard R, Delegado-Bolton R, Oyen WJG, et al. FDG PET/CT: EANM procedure guidelines for tumour imaging: version 2.0 *Eur J Nucl Med Mol Imaging*. 2014;42:328-354.
- [17] Boellaard R, O'Doherty MJ, Weber WA, et al. FDG PET and PET/CT: EANM procedure guidelines for tumour PET imaging: version 1.0 *Eur J Nucl Med Mol Imaging*. 2009;37:181-200.
- [18] Hamil JJ, Sunderland JJ, LeBlanc AK, CJ Kojuma, Wall J, Martin EB. Evaluation of CT-based lean-body SUV *Med Phys*. 2013;40:092504.
- [19] Bland JM, Altman DG. Statistical Methods for Assessing Agreement Between two Methods of Clinical Measurement *Lancet*. 1986;327:307-310.
- [20] Lee J, Koh D, Ong CN. Statistical Evaluation of Agreement Between Two Methods For Measuring a Quantitative Variable *Comput Biol Med*. 1989;19:61-70.

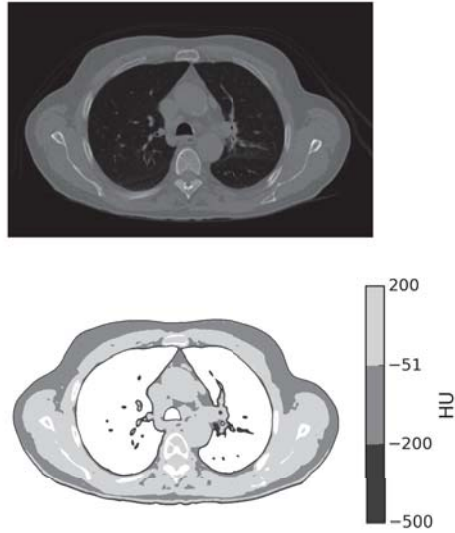


Figure 1: Tissue segmentation in accordance with the CT based method described in Hamil et al. (18). Upper panel showing a CT thorax image in axial projection. Lower panel showing regions segmented out as skin, fat and lean body mass in the Hounsfield Unit ranges $[-500,-201]$, $[-200,-51]$ and $[-50,200]$ respectively.

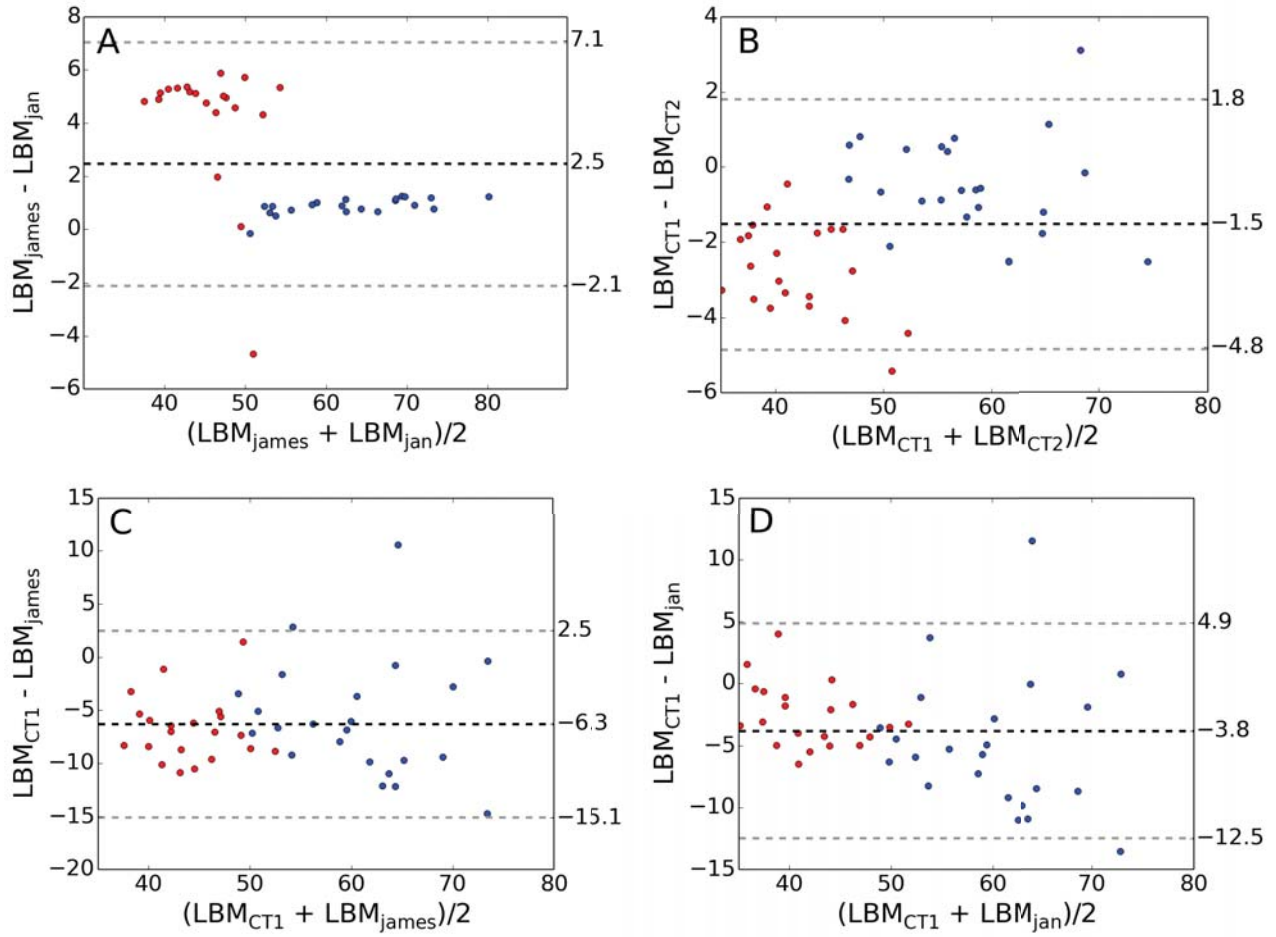


Figure 2: Bland-Altman plots for the comparison of various LBM computation methods. The difference between LBM_{james} and LBM_{jan} , LBM_{CT1} and LBM_{CT2} , LBM_{CT1} and LBM_{james} and LBM_{CT1} and LBM_{jan} are shown in Figure 2A, 2B, 2C, 2D respectively. The dashed black line denotes the mean difference between the compared methods whereas two gray dashed lines denotes the LOA. The blue and red denotes males and females respectively.

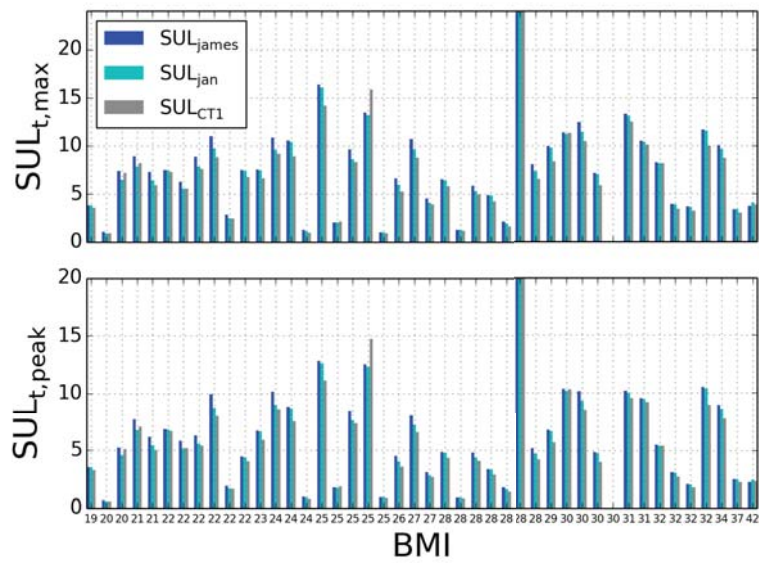


Figure 3: Bar plots for comparison of SUL values illustrating the variations the various LBM calculations can result in for individual tumors. The SUL values of one tumor are given for each patient, and patients are sorted by means of BMI in increasing order. Upper panel show tumor max values and lower panel tumor peak values.

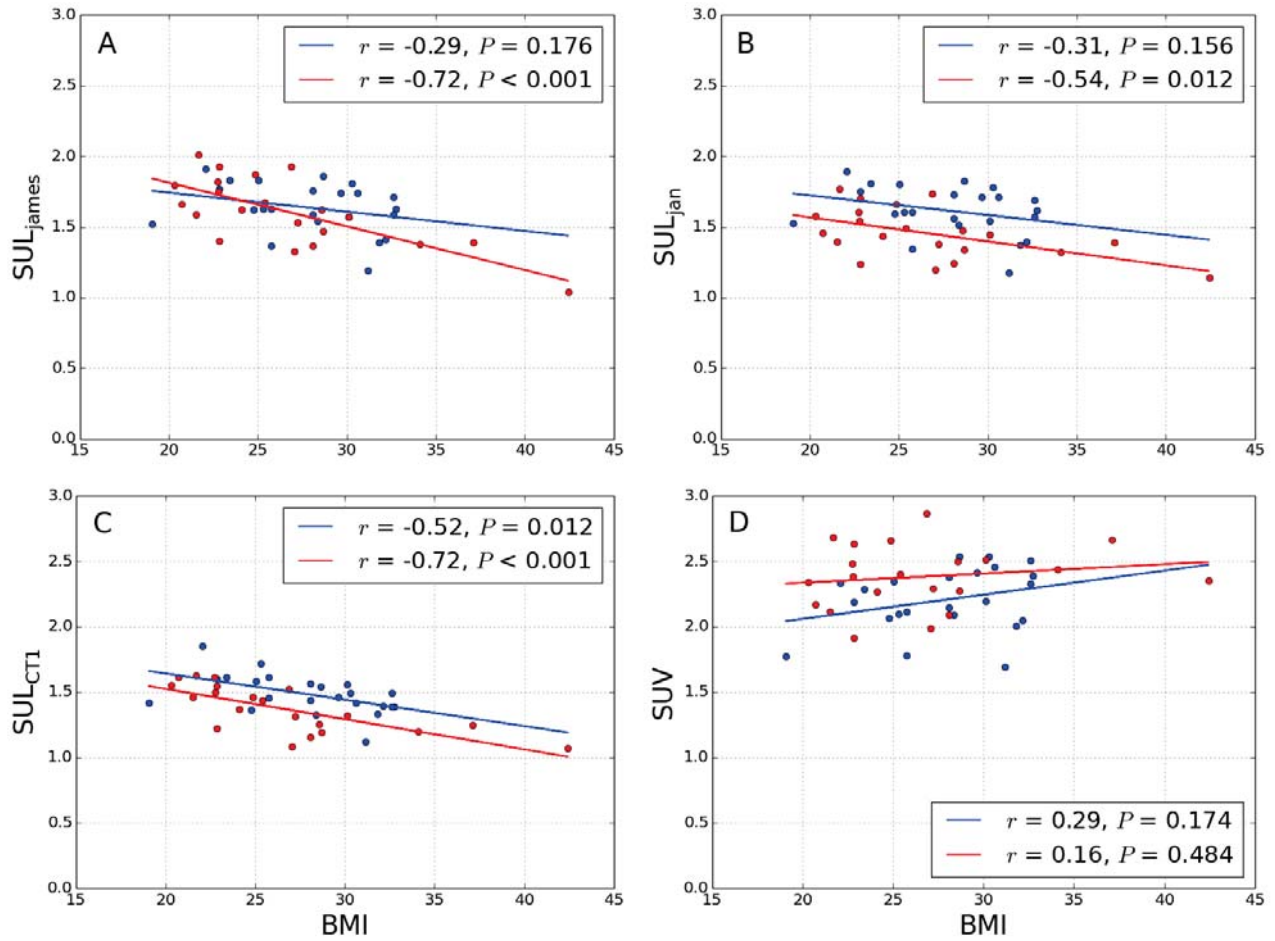


Figure 4: SUL liver values vs. BMI for SUL_{james} , SUL_{jan} and SUL_{CT1} in Figure 4A, 4B and 4C respectively. Figure 4D show SUV liver values vs. BMI. Blue and red dots denotes males and females respectively with associated solid regression lines.

BMI	[18.5, 25.0)	[25.0, 30.0)	[30.0, ∞)
Nb. subjects	15	16	13
Measured	22.4 ± 1.6	27.3 ± 1.4	32.7 ± 4.1
Height[m]	1.66 ± 0.06	1.71 ± 0.07	1.73 ± 0.10
Weight[kg]	62.2 ± 6.1	80.1 ± 9.0	98.0 ± 8.8
Gender bal.(m/f)	5 / 10	9 / 7	9 / 4

Table 1: Patient characteristics.

Method	LBM	ICC, r_I (r_L, r_U)	P
<i>LBM_{james}</i>	55.8 \pm 10.2	0.77 (0.11, 0.91)	< 0.001
<i>LBM_{jan}</i>	53.3 \pm 11.7	0.87 (0.60, 0.94)	< 0.001
<i>LBM_{CT2}</i>	51.0 \pm 9.6	0.98 (0.89, 0.99)	< 0.001
<i>LBM_{CT1}</i>	49.5 \pm 10.4	1	-

Table 2: Intraclass Correlation Coefficients using *LBM_{CT1}* as reference. r_L and r_U denotes the lower and upper limit of the CI.